

Cite this: *RSC Adv.*, 2019, **9**, 39523

# The inhibiting role of hydroxypropylmethylcellulose acetate succinate on piperine crystallization to enhance its dissolution from its amorphous solid dispersion and permeability

Yueyi Deng, <sup>1\*</sup>a Qi Liang,<sup>a</sup> Yiru Wang,<sup>a</sup> Xiaolan Zhang,<sup>a</sup> Chengyun Yan<sup>a</sup> and Yulin He<sup>\*b</sup>

The purpose of this study was to demonstrate that inhibiting crystallization by HPMCAS played a key role in enhancing dissolution and absorption of piperine (Pip) from its amorphous solid dispersion (ASD). Nucleation induction time and supersaturation tests were used to evaluate the ability of the polymers to inhibit crystallization of Pip. The prepared solid dispersions were characterized by DSC and FTIR. The dissolution rate of Pip from its ASDs was assayed by a dissolution test. Pip permeability was investigated by single-pass intestinal perfusion studies. The order of the ability of polymers to inhibit Pip crystallization was HF > MF > LF > L100-55. The best inhibition effect of HF can be attributed to its hydrophobicity and steric hindrance. Pip is amorphous in polymer matrices when the ratio of Pip/HPMCAS is lower than 1 : 1 and Pip/L100-55 is lower than 3 : 1. IR spectra show that there are hydrogen bonds between the amide groups of Pip and the carboxyl groups of polymer. The order of the ability of polymers to enhance Pip dissolution is HF > MF > LF > L100-55, which coincided with the ability of polymers to inhibit Pip crystallization. Increased apparent permeability via HF-induced supersaturation and decreased apparent permeability via solubilization with L100-55 are demonstrated. Nucleation induction time and supersaturation tests may be used to screen appropriate polymers for preparing ASDs.

Received 11th October 2019  
Accepted 24th November 2019

DOI: 10.1039/c9ra08283b

rsc.li/rsc-advances

## Introduction

The number of poorly water-soluble candidate drugs has increased rapidly in the past few decades. It is estimated that more than 90% of the compounds in drug discovery pipelines are poorly water-soluble.<sup>1,2</sup> Low solubility or dissolution rate will significantly reduce the absorption and oral bioavailability of a drug. Therefore, improving the solubility of the poorly water-soluble drugs has become one of the major challenges in the drug formulation field.<sup>3,4</sup>

Many formulation techniques, such as solid phase lipid nanoparticles, self-emulsifying delivery systems, formation of co-crystal and micelles, are being used to increase the solubility of the poorly water-soluble drugs.<sup>5–7</sup> However, low drug loading limits the use of these technologies. In recent years, amorphous solid dispersion (ASD), which can increase the solubility of a large number of the poorly water-soluble drugs with different

physical and chemical properties, has aroused strong concern.<sup>8–10</sup>

ASD is defined as a situation where one or more than one drug is dispersed in polymer matrix and exhibits amorphous state in the solid dispersion. The amorphous drug with high energy has larger solubility compared to its crystal form. ASD has high drug loading, and the water-soluble polymer matrixes used for ASD are derived from pharmaceutical excipients with high safety. It has been reported that the solubility enhancement by solubilizer reduces the transmembrane transport of drug, but the supersaturated solution (the apparent solubility of drug,  $C_{app}$ , is higher than the equilibrium solubility,  $C_s$ ) formed by dissolution of ASD, enhances drug transmembrane transport for its higher chemical potential.<sup>11–13</sup> Unfortunately, the supersaturated solution tends to crystallize due to its high energy state. The extensive research have shown that some water-soluble polymer excipients, such as HPMCAS, HPMC and PVP, play a key role on maintaining the supersaturated solutions as precipitation inhibitors.<sup>14–17</sup> Therefore, the rational selection of polymer used for ASD is very important for developing ASD formulation successfully.

Pip is an alkaloid and extracted from black pepper. It has exhibited anti-inflammatory, antioxidant, anti-tumor and

<sup>a</sup>School of Pharmacy, Guilin Medical University, 541004 Guilin, Guangxi, People's Republic of China. E-mail: dengyyqust@hotmail.com

<sup>b</sup>School of Basic Medical, Guilin Medical University, 541004 Guilin, Guangxi, People's Republic of China. E-mail: 418497164@qq.com



antidepressant activities.<sup>18–20</sup> In addition, it is an inhibitor of glucuronidation and an P-gp efflux transporter located on the gastrointestinal epithelial cells, which can be used to improve the bioavailability of many drugs. It has been reported that Pip can effectively improve the bioavailability of curcumin as an oral absorption enhancer recently.<sup>21–23</sup> As a drug, Pip is not able to reach a high concentration in the gastrointestinal tract due to its low solubility and rapid crystallization in aqueous solution, so its therapeutic role is limited.<sup>24</sup>

In this study, the water-soluble polymers HPMCAS with different carboxyl content (HF, MF, and LF) and Eudragit L100-55 were chosen as matrixes to prepare the amorphous solid dispersions of Pip. Pip is weak base and the polymers with carboxyl groups show acidity in aqueous media, so there will be acid-base interactions between Pip and the polymers. These polymers may maintain supersaturated Pip solution through these interactions and enhance dissolution of Pip. By measuring the induction time of nucleation and supersaturation test, the effect of inhibiting Pip crystallization by these polymers was investigated. The ASDs of Pip were prepared by the solvent evaporation method and characterized by DSC and IR. The dissolution profiles of the ASDs of Pip were investigated by dissolution test. Permeability of Pip solution in the absence or presence of polymer was assayed by *in situ* single-pass intestinal perfusion studies.

## Materials and methods

### Materials

Pip (97%) was purchased from Sinopharm Chemical Reagent Co., Ltd (Shanghai, China). HF (degree of substitution (DS) (acetyl) = 0.67, DS (succinoyl) = 0.18), MF (DS (acetyl) = 0.52, DS (succinoyl) = 0.26) and LF (DS (acetyl) = 0.48, DS (succinoyl) = 0.37) were obtained from Shin-Etsu Chemical Company (Tokyo, Japan). L100-55 (1 : 1 methacrylic acid and methyl methacrylate copolymer) was donated by Evonik Industries AG (Darmstadt, Germany). All other reagents were analytical grade and used as received.

### Solubility measurement

The selected polymers were predissolved in 100 mM pH 6.8 PBS at a concentration of 0.63 mg mL<sup>-1</sup>. The equilibrium solubility of Pip was determined in the absence and presence of polymer. An excess amount of Pip was added to 20 mL PBS and stirred at 350 rpm and 37 °C for 24 h. After filtration through a 0.22 µm cellulose ester membrane filter, the drug concentration in the filtrate was obtained by HPLC.

### Supersaturation test

200 µL DMSO solution of Pip (56 mg mL<sup>-1</sup>) was added to 80 mL pH 6.8 PBS with or without polymer (0.63 mg mL<sup>-1</sup>) under stirring at 37 °C. The concentration of DMSO was very low and had no effect on the solubility of Pip. 3 mL of solution was sampled and filtered through 0.22 µm cellulose ester membrane at 5, 10, 15, 30, 45, 60, 90, 120 and 240 min after mixing. The concentration of Pip was determined by HPLC. The

ability of polymer to maintain supersaturation could be evaluated by supersaturation parameters (SSP).<sup>25</sup> As shown in Fig. 1,  $C_0$  is the initial concentration of Pip, and  $C_R(t)$  is Pip concentration at the  $t$  moment in the absence of polymer.  $C_a(t)$  or  $C_b(t)$  is Pip concentration at the  $t$  moment in the presence of polymer. SSP can be calculated by the following formula:

$$\text{SSP} = \frac{A_{C_0 C_R(t) C_0(t)} - A_{C_0 C(t) C_0(t)}}{A_{C_0 C_R(t) C_0(t)}} \times 100\%$$

### Nucleation induction time measurement

Nucleation induction time ( $t_{\text{ind}}$ ), which is used to characterize crystallization kinetics, is defined as the required time that the small crystals with a detectable size begin to form in supersaturated solution.  $t_{\text{ind}}$  can be determined by the abrupt increase in intensity of light scattered (extinction) from drug solution. Extinction at 430 nm for Pip is detected by a UV/vis spectrometer (UV-1200, Shimadzu, Japan) and Pip has no absorbance at this wavelength. Supersaturated drug solutions were prepared by the solvent-shift method. 0.5 mL DMSO solution of Pip (4 mg mL<sup>-1</sup>) was added to 200 mL pH 6.8 PBS in the absence and presence of predissolved polymers (0.63 mg mL<sup>-1</sup>) under stirring at 350 rpm. After mixing, 0.5 mL solution was sampled and measured by the UV/vis spectrometer at a certain time interval.

### Preparation of solid dispersions

Pip/polymer mixtures (1 g, w/w: 3 : 1, 1 : 1, 1 : 3 and 1 : 9) were dissolved in 100 mL of ethanol/dichloromethane mixtures (v/v: 1 : 1). The solvent was removed using rotary evaporation at 60 °C and the remaining solid was dried in vacuum for 24 h. Solid dispersions were ground with a mortar and pestle and passed through a 60 mesh sieve.

### Differential scanning calorimetry (DSC)

The thermal analysis was carried out using a DSC (214, Netzsch, Germany). A 2–5 mg solid dispersion sample was loaded in an aluminum pan and sealed by a lid with a pin hole, taking an empty aluminum pan as reference. Samples were heated from 35 °C to 200 °C at a heating rate of 10 °C min<sup>-1</sup> in an atmosphere of nitrogen with a flow rate of 20 mL min<sup>-1</sup>. DSC curves were analyzed using Proteus software (Netzsch, Germany).

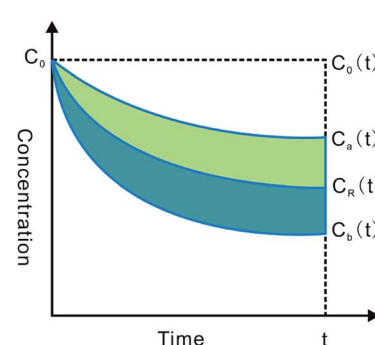


Fig. 1 Schematic diagram of supersaturated parameters.



## FTIR spectroscopy

FTIR spectra were recorded in the range of 400–4000  $\text{cm}^{-1}$  on a Nicolet 170SX spectrometer with pressed KBr pellets. 128 scans were collected for each sample, and the resolution was 4  $\text{cm}^{-1}$ .

## Dissolution studies

Pip release profiles were investigated under non-sink conditions. 320 mg Pip/polymer 1 : 9 ASDs were added to 200 mL pH 6.8 PBS with stirring at 150 rpm and 37 °C. Samples of 2 mL were withdrawn at predetermined time intervals (1, 5, 10, 20, 30, 45, 60, 90, 120, 180, 240 min and 24 h) and replaced with 2 mL fresh dissolution medium. The aliquots were filtered through 0.22  $\mu\text{m}$  cellulose ester membrane and Pip concentration in the filtrate was determined by HPLC. Experiments were performed in triplicate and the average values with standard deviations were presented for all dissolution profiles.

## *In situ* single-pass intestinal perfusion studies

All animal experiments were performed in compliance with the NIH guidelines for the Care and Use of Laboratory Animals (NIH Publication, Eighth edition, 2011) and were approved by the Experimental Animal Ethics Committee of the Guilin Medical University (Guangxi, China). Male albino Sprague-Dawley rats weighing 250–300 g were used for all perfusion studies. Prior to each experiment, the rats were fasted for 12–18 h with free access to water.

The experimental procedure for the single-pass perfusions followed previous reports.<sup>26–28</sup> Rats were anesthetized by 1  $\text{mL kg}^{-1}$  ketamine–xylazine solution (9% : 1%) and placed alongside of a infrared light to keep normal body temperature. A 3–4 cm incision was made along the midline of abdomen. A proximal jejunal segment of approximately 10 cm was carefully exposed and cannulated on two ends with flexible PVC tubing. The exposed intestinal segment was kept moist with the wetting wound dressing.

The supersaturated solution (3 times equilibrium solubility, according to the ability of HF to inhibit crystallization) were prepared by adding 4 mg  $\text{mL}^{-1}$  DMSO solution of Pip to 200 mL 50 mM pH 6.8 PBS containing HF (0.63 mg  $\text{mL}^{-1}$ ) under stirring at 350 rpm. Pip was dissolved in 200 mL 50 mM pH 6.8 PBS containing L100-55 (0.63 mg  $\text{mL}^{-1}$ ) to obtain the concentration of 60  $\mu\text{g mL}^{-1}$ . All perfusate solutions were kept at 37 °C in a water bath and were pumped through the isolated intestinal segment (HL-2, HUXI, China). The intestinal segment was first rinsed with blank perfusion buffer at a flow rate of 0.5  $\text{mL min}^{-1}$  until any residual debris were cleaned out. The perfusate solutions containing Pip were then pumped through the intestinal segment for 1 h at a flow rate of 2.5  $\text{mL min}^{-1}$  in order to reaching steady state conditions. In another hour, samples were collected at an interval of 15 min in a pre-weighed glass tube. Drug concentration in perfusion samples at different time points and original drug solution were immediately assayed by HPLC. At the end of the experiment, animals were euthanized with saturated potassium chloride solution by

intracardiac injection. The length and radius of each intestinal segment was accurately measured.

Water absorption was determined by the gravimetric method. The outlet concentration of Pip was corrected by the following equation:

$$C'_{\text{out}} = C_{\text{out}} \times \frac{Q_{\text{out}}}{Q_{\text{in}}}$$

where  $C'_{\text{out}}$  is the corrected outlet concentration of Pip;  $C_{\text{out}}$  is the outlet concentration of Pip;  $Q_{\text{out}}$  and  $Q_{\text{in}}$  are the outlet and inlet perfusate flux, respectively.

The effective permeability ( $P_{\text{eff}}$ ) through the rat gut wall was determined by the following equation:

$$P_{\text{eff}} (\text{cm s}^{-1}) = \frac{-Q_{\text{in}} \ln \left( C'_{\text{out}} / C_{\text{in}} \right)}{2\pi RL}$$

where  $Q_{\text{in}}$  is the inlet perfusate flux;  $C_{\text{in}}$  is the inlet concentration of Pip;  $R$  is the radius of the intestinal segment, and  $L$  is the length of the intestinal segment.

## High performance liquid chromatography (HPLC)

Pip concentration was determined using an Agilent 1100 HPLC system (Agilent Technologies, Santa Clara, CA). Pip was detected by UV absorbance at 343 nm. A Zobrax SB-C18 column (150  $\times$  4.6 mm<sup>2</sup>, 5  $\mu\text{m}$ ) was applied to chromatographic separation. The mobile phase consists of phosphate buffer (pH 6.8) (30%) and methanol (70%). The flow rate was 1  $\text{mL min}^{-1}$  and the injection volume was 20  $\mu\text{L}$ .

## Statistical analysis

All *in vitro* experiments were performed in triplicate, and all animal experiments were  $n = 4$ . The data are presented as the mean  $\pm$  the standard deviation (SD). Statistically significant differences of  $P_{\text{eff}}$  were determined by analysis of variance (ANOVA) and Tukey tests, and a  $p$  value of less than 0.05 was termed significant.

## Results and discussion

### Effect of polymer on equilibrium solubility of Pip

The equilibrium solubility of crystalline Pip is 20  $\mu\text{g mL}^{-1}$ , and the apparent solubility of Pip increases in the presence of polymer (Fig. 2). The selected polymers have solubilization effect on Pip, and the order of solubilization is L100-55 > LF > MF  $\geq$  HF. There is a direct correlation between solubilization ability and carboxyl content in polymer (the order of carboxyl content of polymer: L100-55 > LF > MF > HF). These results indicate that there is an acid–base interaction between polymer and Pip, which improves the equilibrium solubility of Pip.

### The maintaining role of polymer on the supersaturated solution of Pip

As shown in Fig. 3, Pip precipitated rapidly and the concentration decreased to 26.4  $\mu\text{g mL}^{-1}$  in 1 min, indicating that almost no supersaturation was formed. SSP can be used to evaluate the



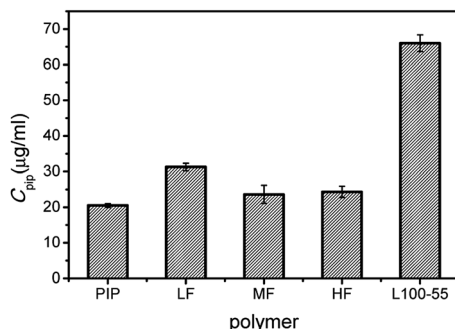


Fig. 2 The equilibrium solubility of Pip in the presence or absence of polymers.

ability of polymer to maintain supersaturation. From Table 1, the order of stabilizing Pip supersaturation solutions is HF > MF > LF > L100-55, which is opposite to the solubilization role. L100-55 can enhance Pip solubility, but it has little role on maintaining supersaturation. It can be seen from Fig. 3 that HPMCAS can inhibit crystallization of Pip from the supersaturated solutions and significantly prolong supersaturation time, acting as “parachutes”. The inhibition role of polymer is carried out by thermodynamics or kinetics.<sup>29,30</sup> The thermodynamic way can reduce the crystallization rate by a decrease of supersaturation degree with improving solubility. Kinetics inhibition refers to the reduced rates of nucleation and crystal growth. According to solubility studies, HPMCAS has a little effect on Pip solubility, so the crystallization inhibition role of HPMCAS is based on kinetics. The factors affecting the inhibition ability of polymer include drug–polymer interaction, steric hindrance of polymer, hydrophobicity and solution viscosity, *etc.*<sup>31–33</sup> HPMCAS has a better inhibition role than L100-55, which may be ascribed to steric hindrance of HPMCAS. HF is the most effective in the inhibition of crystallization of Pip, which may be attributed to the strong hydrophobic interactions between Pip and HF (HF is the most hydrophobic when compared to MF and HF due to its low carboxyl content).

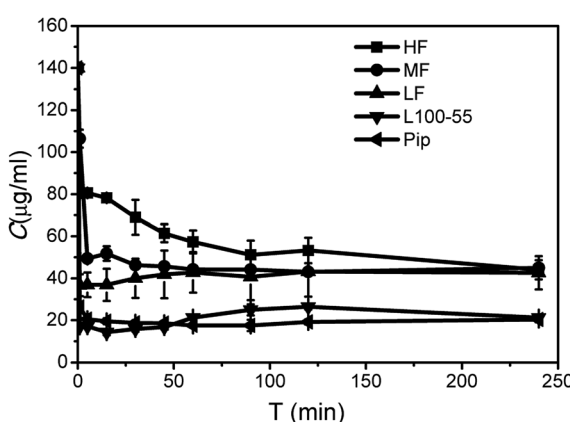


Fig. 3 Desaturated curves of Pip supersaturated solutions in the presence or absence of polymers.

Table 1 SSP values in the supersaturation test

SSP/%	MF	HF	LF	L100-55
Pip	22	30	19	1.4

Following the supersaturation experiment, the precipitate was investigated by optical microscopy. Pip crystals have long needle to rod-like morphology with high aspect ratio in the absence of polymer (Fig. 4A). The crystal morphology doesn't change in the presence of L100-55 (Fig. 4B), indicating L100-55 has little effect on the process of nucleation and crystal growth. This result is in agreement with the supersaturation result. Pip crystal surfaces become rough and have lower aspect ratio in the presence of HPMCAS (Fig. 4C–E). Rough surfaces reveal that crystals grow by diffusion mechanism, in which the diffusion of Pip molecules is limited by large steric hindrance of HPMCAS. Pip crystals have plate-like morphology and the lowest aspect ratio in the presence of HF, indicating that there are the strongest interactions between Pip and HF.<sup>34</sup> The extent to

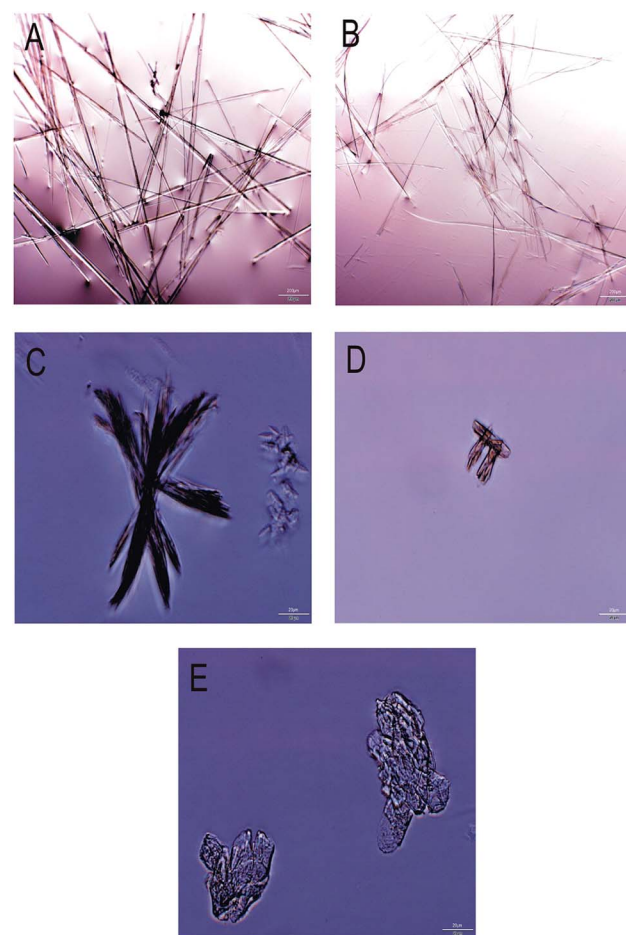


Fig. 4 Optical microscopic images of Pip crystal in the presence and absence of polymers ((A) no polymer; (B) L100-55; (C) LF; (D) MF; (E) HF).



which the aspect ratio of crystals is modified correlates with the crystallization inhibition ability of these polymers.

### Inhibition of nucleation process of Pip by polymer

Nucleation behavior of Pip from the supersaturated solution was investigated in the presence or absence of polymer. Nucleation can be quantified by measuring the time that small crystal particles begin to be detected, which is known as  $t_{ind}$ . As shown in Fig. 5, the  $t_{ind}$  of Pip nucleation is 2 min in the absence of polymer and 5, 8, 10, 40 min in the presence of L100-55, LF, MF and HF, respectively. So the order of inhibiting nucleation ability of polymer is HF > MF > LF > L100-55. This order is consistent with the ability of polymer to maintain Pip supersaturated solution, which suggests that the inhibition of polymer on Pip crystallization may be ascribed to the inhibition of nucleation process of crystallization. The ability of nucleation inhibition of polymer is determined by drug–water–polymer interaction.<sup>35</sup> It is very important that polymer has similar hydrophobicity to drug for nucleation inhibition. Too low or high hydrophobicity of polymer is unfavourable to nucleation inhibition.<sup>36</sup> HF has the most effective inhibition on Pip nucleation, indicating that HF has close hydrophobicity to Pip. The stronger hydrophobic interaction between Pip and HF disrupt Pip aggregates, which can further assemble into small crystals with order structure. The nucleation inhibition ability of LF, MF and HF is higher than that of L100-55, which indicates that HPMCAS with large steric hindrance can prevent the assembly of Pip molecules more effectively than L100-55.

### Characterization of the ASDs

The DSC curves of the prepared solid dispersions are shown in Fig. 6. As shown in Fig. 6B, pure Pip has one melting peak at

131.1 °C. In Fig. 6A, there are no melting peaks of Pip for the 1 : 3 and 1 : 9 Pip/polymer solid dispersions, which indicates that Pip is dispersed amorphously in polymer and the ASDs of Pip are obtained. If a solid dispersion shows only one  $T_g$ , then the drug and the polymer have good compatibility.<sup>37–39</sup> All the 1 : 3 and 1 : 9 Pip/HPMCAS solid dispersions show one  $T_g$ , while 1 : 3 Pip/L100-55 has two  $T_g$ s, indicating that HPMCAS has better compatibility with Pip than L100-55. The two  $T_g$ s of Pip/HF solid dispersions are closer to each other than those of the Pip/MF and Pip/LF solid dispersions, which suggest that stronger interactions exist between HF and Pip. Two  $T_g$ s of 1 : 3 Pip/L100-55 solid dispersion are closest to each other, which may suggest that Pip is distributed better in L100-55 than HPMCAS during preparation for good solubility of L100-55 in the solvents.

The drug loading capacity of solid dispersion is the maximum amount of drug that can be amorphous in polymer carrier.<sup>40</sup> The 1 : 2 solid dispersions of HF, MF and LF have no endothermic peaks and the 1 : 1 solid dispersions show melting peaks between 120 °C and 130 °C (Fig. 6B), which indicates that the maximum drug loading of HF, MF and LF is between 33% and 50%. The 3 : 1 solid dispersion of L100-55 has a very small melting peak at 126.2 °C (the peak can not be seen in Fig. 6C) and there is no endothermic peak when the ratio of Pip and L100-55 is 1 : 1 (Fig. 6B), which shows that the maximum drug loading of L100-55 is close to 75%. The melting peak area of 1 : 1 solid dispersions of HF, MF and LF are 1.56, 1.381 and 0.4073 J g<sup>-1</sup> respectively, which shows that the order of drug loading abilities of polymers under the same condition of preparation is L100-55 > LF > HF > MF. L100-55 has the highest drug loading capacity may be attributed to better Pip distribution in L100-55 than HPMCAS during preparation for good

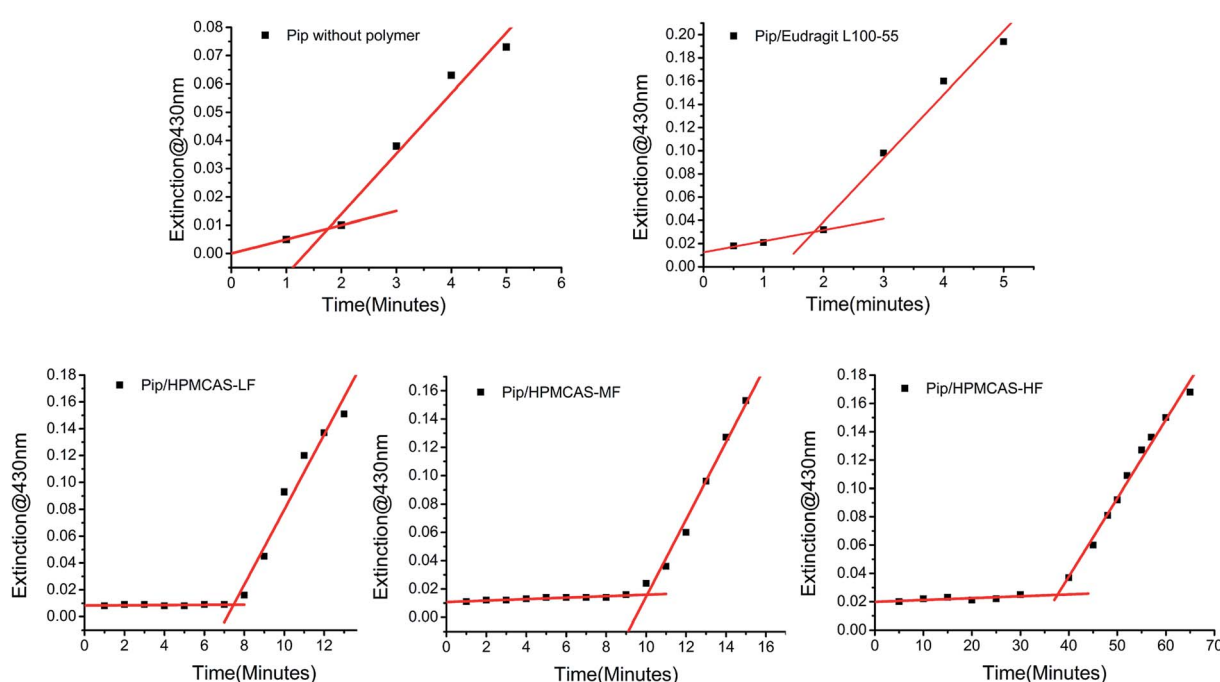


Fig. 5 The change of extinction with time of Pip supersaturated solutions in the presence or absence of polymers.

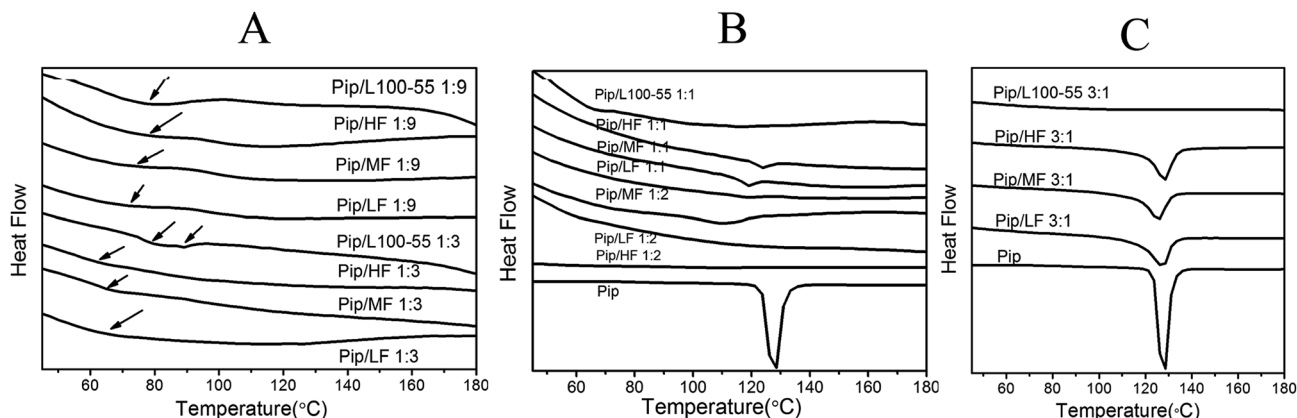


Fig. 6 The DSC curves of 1 : 9 and 1 : 3 Pip solid dispersions (A); the DSC curves of 1 : 1 Pip solid dispersions (B); the DSC curves of 3 : 1 solid dispersions (C).

solubility of L100-55 in the solvents. The melting points of solid dispersions decrease compared with pure Pip (Fig. 6B and C), indicating that there are interactions between Pip and polymers, which disrupt crystallization of Pip.<sup>41</sup> With the increase in drug content, the melting points of solid dispersions are closer to that of Pip.

The FTIR spectra of dispersion solids are shown in Fig. 7. For crystalline Pip, the strong band at  $1583\text{ cm}^{-1}$  is ascribed to benzene ring stretching and the peak at  $1634\text{ cm}^{-1}$  is C=O-N absorption. For amorphous Pip, these peaks shift to 1587 and  $1636\text{ cm}^{-1}$  respectively, which shows the change of the molecular environment of these groups. The bands of amorphous Pip

are more smooth and broad than those of crystalline Pip. When the ratio of drug and polymer (HF, MF and LF) is smaller than 3 : 1, the shape and wavenumber of the peaks of the solid dispersions are similar to those of amorphous Pip, suggesting that these solid dispersions are amorphous. The 3 : 1 solid dispersions of HF, MF and LF exhibit the bands of crystalline Pip at  $1583$  and  $1634\text{ cm}^{-1}$ , showing the presence of crystalline Pip in these solid dispersions. These results are in agreement with the DSC results. The peaks around  $1740\text{ cm}^{-1}$  are absorption bands of polymer carbonyl groups and these peaks shift compared to pure polymers, which confirms Pip–polymer interactions.<sup>42</sup> For Pip/L100-55 solid dispersions, the shoulder

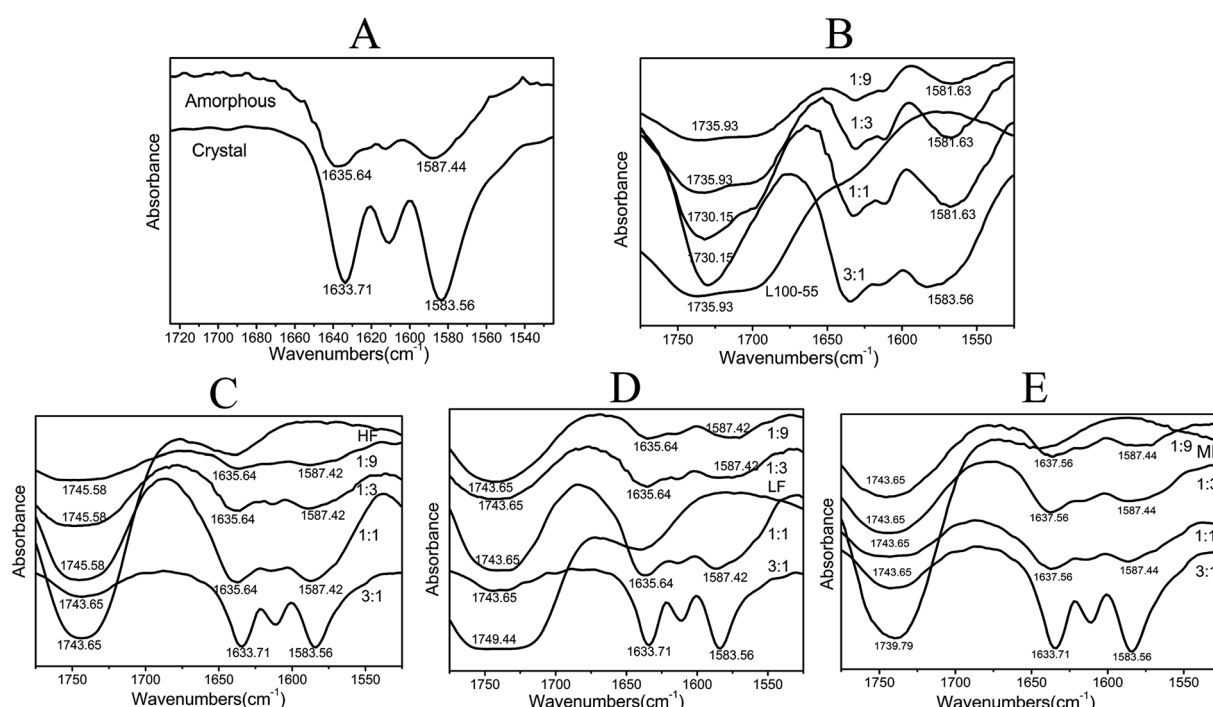


Fig. 7 (A) is IR spectra of crystal Pip and amorphous Pip; (B), (C), (D) and (E) are IR spectra of Pip/L100-55, Pip/HF, Pip/LF, Pip/MF solid dispersions with different proportions respectively.



peaks at  $1715\text{ cm}^{-1}$  disappear and the peaks around  $1700\text{--}1740\text{ cm}^{-1}$  become stronger as drug content increase, indicating stronger Pip-polymer interactions.

### Drug release profiles

As shown in Fig. 8, the prepared ASDs can enhance the dissolution of Pip. The dissolution rate of pure Pip was very slow and only 14.5% of Pip release was reached in 3 h. The dissolution rate and drug release of the ASDs were higher than that of pure Pip. During dissolution, we found that the ASDs were immediately mixed with the dissolution medium and the solution became cloudy, while the pure Pip floated on the surface of the dissolution medium for a long time. These results indicate that the polymer carriers enhance the wettability of Pip and improve Pip release.<sup>43</sup> Release from the Pip/MF, Pip/LF and Pip/L100-55 ASDs was very fast, reaching 59% within 10 min, 57.8% within 15 min and 32% within 5 min respectively, while release from the Pip/HF ASD was slow and reached 59.6% within 3 h. These results may be related to the dissolution rate of polymer, the order of which in the dissolution medium is L100-55 > LF > MF > HF. It can be found from Fig. 8 that L100-55, LF and MF can accelerate the dissolution rate of Pip, but these polymers can not maintain a high Pip concentration in 24 h. HF can not only increase the dissolution rate of Pip, but also maintain a higher drug concentration within 24 hours. We can obtain the order of the ability of polymer to enhance the dissolution of Pip is HF > MF > LF > L100-55, which is consistent with the ability of polymer to inhibit Pip nucleation and maintain the supersaturated solution of Pip. These results indicate that inhibiting Pip crystallization by polymer plays a key role for enhancing Pip dissolution.

### Effect of supersaturation on permeability

Pip permeability from saturated solution ( $20\text{ }\mu\text{g mL}^{-1}$ ), a solution containing L100-55 ( $60\text{ }\mu\text{g mL}^{-1}$ ) and a supersaturated solution in the presence of HF ( $60\text{ }\mu\text{g mL}^{-1}$ ) was investigated by single-pass intestinal perfusion studies. As shown in Fig. 9, the apparent permeability of HF-induced supersaturated solution

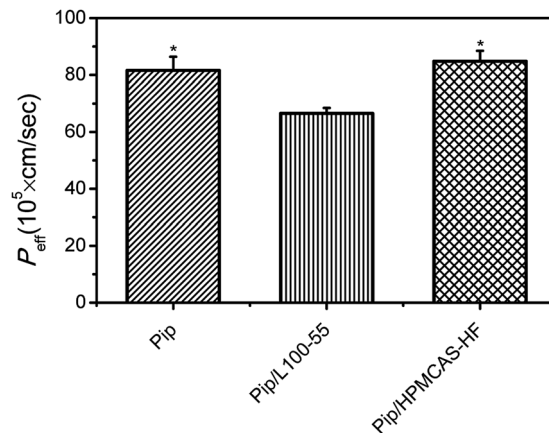


Fig. 9  $P_{\text{eff}}$  of from saturated solution, a solution containing L100-55 and a supersaturated solution in the presence of HF was assayed by single-pass intestinal perfusion studies.  $*p < 0.05$  versus Pip solution. Average  $\pm$  SD;  $n = 4$ .

remained unchanged compared to Pip saturated solution, whereas Pip solution in the presence of L100-55 resulted in decreased apparent permeability. As a result, overall flux increased markedly with increasing apparent solubility *via* supersaturation. It had been reported that increasing apparent solubility *via* cyclodextrins, surfactants, and cosolvents resulted in decreased apparent permeability.<sup>28,44,45</sup> These results show that the solubilization mechanism may affect intestinal absorption. Solubilizers such as cyclodextrins, surfactants, and cosolvents increase aqueous solubility of drug by complexation and micellization, which result in decreased “free” drug available for absorption. As for supersaturation, the high apparent solubility is maintained by kinetically inhibiting crystallization with polymer, resulting in increased “free” fraction of drug with high chemical potential to enhance transmembrane transport. Recently, some polymers with solubilization effect, such as PVP, have been found to decreases the apparent permeability.<sup>46</sup> In our studies, we obtain the similar result that L100-55 with good solubilization role on Pip sacrifice apparent intestinal membrane permeability, which may be attributed to the encapsulation of the drug into L100-55 and the change of the molecular state of Pip in the presence of the acid-base interaction.<sup>46</sup>

### Conclusions

In this paper, HF, MF, LF and L100-55 were used as carriers to prepare ASDs of Pip. Dissolution enhancement by the Pip/HF solid dispersion can be own to the strong nucleation inhibition ability of HF. Compared with the acid-base interaction, hydrophobicity and steric hindrance of polymer are the dominant factors for maintaining the supersaturated solution of Pip. HF-induced supersaturation resulted in increased apparent intestinal membrane permeability, whereas solubilization by L100-55 resulted in decreased apparent permeability. Nucleation induction time and supersaturation test may be used to screen appropriate polymers for ASD formulations.

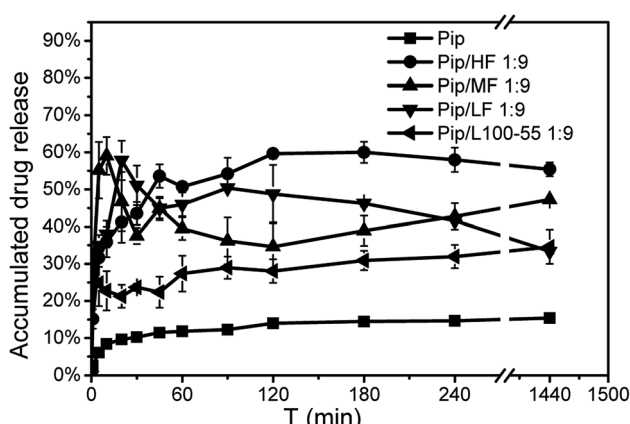


Fig. 8 Dissolution curves of Pip, the 1:9 Pip/L100-55 and Pip/HPMCAS solid dispersions in pH 6.8 PBS.



## Conflicts of interest

There are no conflicts to declare.

## Acknowledgements

The authors would like to acknowledge the research funding from the NSF of Guangxi (grant numbers 2014GXNSFBA118052, 2016GXNSFAA380266).

## References

- 1 L. Di, P. V. Fish and T. Mano, Bridging solubility between drug discovery and development, *Drug Discovery Today*, 2012, **17**, 486–495.
- 2 H. D. Williams, N. L. Trevaskis, S. A. Charman, R. M. Shanker, W. N. Charman, C. W. Pouton and C. J. Porter, Strategies to address low drug solubility in discovery and development, *Pharmacol. Rev.*, 2013, **65**(1), 315–499.
- 3 H. Yan and H. Chris, Amorphous solid dispersions: utilization and challenges in drug discovery and development, *J. Pharm. Sci.*, 2015, **104**, 3237–3258.
- 4 L. N. V. Chau, P. Chulhun and B. J. Lee, Current trends and future perspectives of solid dispersions containing poorly water-soluble drugs, *Eur. J. Pharm. Sci.*, 2013, **85**, 799–813.
- 5 Y. Kawabata, K. Wada, M. Nakatani, S. Yamada and S. Onoue, Formulation design for poorly water-soluble drugs based on biopharmaceutics classification system: Basic approaches and practical applications, *Int. J. Pharm.*, 2011, **420**(1), 1–10.
- 6 K. Kawakami, Modification of physicochemical characteristics of active pharmaceutical ingredients and application of supersaturatable dosage forms for improving bioavailability of poorly absorbed drugs, *Adv. Drug Delivery Rev.*, 2012, **64**(6), 480–495.
- 7 R. Shegokar and R. H. Muller, Nanocrystals: Industrially feasible multifunctional formulation technology for poorly soluble actives, *Int. J. Pharm.*, 2010, **399**(1–2), 129–139.
- 8 D. N. Bikiaris, Solid dispersions, part I: Recent evolutions and future opportunities in manufacturing methods for dissolution rate enhancement of poorly water-soluble drugs, *Expert Opin. Drug Delivery*, 2011, **8**(11), 1501–1519.
- 9 A. T. Serajuddin, Solid dispersion of poorly water-soluble drugs: Early promises, subsequent problems, and recent breakthroughs, *J. Pharm. Sci.*, 1999, **88**(10), 1058–1066.
- 10 L. Yu, Amorphous pharmaceutical solids: Preparation, characterization and stabilization, *Adv. Drug Delivery Rev.*, 2001, **48**(1), 27–42.
- 11 M. di Cagno and B. Luppi, Drug “supersaturation” states induced by polymeric micelles and liposomes: A mechanistic investigation into permeability enhancements, *Eur. J. Pharm. Sci.*, 2013, **48**(4–5), 775–780.
- 12 J. M. Miller, A. Beig, R. A. Carr, J. K. Spence and A. Dahan, A win-win solution in oral delivery of lipophilic drugs: Supersaturation via amorphous solid dispersions increases apparent solubility without sacrifice of intestinal membrane permeability, *Mol. Pharm.*, 2012, **9**(7), 2009–2016.
- 13 S. A. Raina, G. G. Z. Zhang, D. E. Alonzo, J. Wu, D. Zhu, N. D. Catron, Y. Gao and L. S. Taylor, Enhancements and limits in drug membrane transport using supersaturated solutions of poorly water-soluble drugs, *J. Pharm. Sci.*, 2014, **103**(9), 2736–2748.
- 14 D. B. Warren, H. Benameur, C. J. H. Porter and C. W. Pouton, Using polymeric precipitation inhibitors to improve the absorption of poorly water-soluble drugs: A mechanistic basis for utility, *J. Drug Targeting*, 2010, **18**(10), 704–731.
- 15 M. J. Jackson, U. S. Kestur, M. A. Hussain and L. S. Taylor, Characterization of supersaturated danazol solutions—impact of polymers on solution properties and phase transitions, *Pharm. Res.*, 2016, **33**, 1276–1288.
- 16 T. Xie and L. S. Taylor, Dissolution performance of high drug loading celecoxib amorphous solid dispersions formulated with polymer combinations, *Pharm. Res.*, 2016, **33**, 739–750.
- 17 C. Liu, Z. Chen, Y. J. Chen, J. Lu, Y. Li, S. J. Wang, G. L. Wu and F. Qian, Improving oral bioavailability of sorafenib by optimizing the “spring” and “parachute” based on molecular interaction mechanisms, *Mol. Pharmaceutics*, 2016, **13**, 599–608.
- 18 S. Kumar, V. Singhal, R. Roshan, A. Sharma, G. W. Rembhokar and B. Ghosh, Piperine inhibits TNF-alpha induced adhesion of neutrophils to endothelial monolayer through suppression of NF- $\kappa$ B and Ikappa B kinase activation, *Eur. J. Pharmacol.*, 2007, **575**, 177–186.
- 19 K. A. Naidu and N. B. Thippeswamy, Inhibition of human low density lipoprotein oxidation by active principles from spices, *Mol. Cell. Biochem.*, 2002, **229**, 19–23.
- 20 S. Li, C. Wang, M. Wang, W. Li, K. Matsumoto and Y. Tang, Antidepressant like effects of piperine in chronic mild stress treated mice and its possible mechanisms, *Life Sci.*, 2007, **80**, 1373–1381.
- 21 G. Shoba, D. Joy, T. Joseph, M. Majeed, R. Rajendran and P. S. Srinivas, Influence of piperine on the pharmacokinetics of curcumin in animals and human volunteers, *Planta Med.*, 1998, **64**, 353–356.
- 22 J. Shaikh, D. D. Ankola, V. Beniwal, D. Singh and M. N. V. Ravi Kumar, Nanoparticle encapsulation improves oral bioavailability of curcumin by at least 9-fold when compared to curcumin administered with piperine as absorption enhancer, *Eur. J. Pharm. Sci.*, 2009, **37**, 223–230.
- 23 S. Singh, S. Jamwal and P. Kumar, Piperine enhances the protective effect of curcumin against 3-NP induced neurotoxicity: possible neurotransmitters modulation mechanism, *Neurochem. Res.*, 2015, **40**, 1758–1766.
- 24 M. Pachauri, E. D. Gupta and P. C. Ghosh, Piperine loaded PEG-PLGA nanoparticles: preparation, characterization and targeted delivery for adjuvant breast cancer chemotherapy, *J. Drug Delivery Sci. Technol.*, 2015, **29**, 269–282.
- 25 Y. Chen, C. Liu, Z. Chen, C. Su, M. Hageman, M. Hussain, R. Haskell, K. Stefanski and F. Qian, Drug–polymer–water interaction and its implication for the dissolution performance of amorphous solid dispersions, *Mol. Pharmaceutics*, 2015, **12**(2), 576–589.



26 A. Dahan, J. M. Miller, J. M. Hilfinger, S. Yamashita, L. X. Yu, H. Lennernas and G. L. Amidon, High-permeability criterion for BCS classification: Segmental/pH dependent permeability considerations, *Mol. Pharmaceutics*, 2010, **7**(5), 1827–1834.

27 A. Dahan and G. L. Amidon, Segmental dependent transport of low permeability compounds along the small intestine due to P-glycoprotein: The role of efflux transport in the oral absorption of BCS class III drugs, *Mol. Pharmaceutics*, 2009, **6**(1), 19–28.

28 J. M. Miller, A. Beig, R. A. Carr, J. K. Spence and A. Dahan, A win–win solution in oral delivery of lipophilic drugs: supersaturation *via* amorphous solid dispersions increases apparent solubility without sacrifice of intestinal membrane permeability, *Mol. Pharmaceutics*, 2012, **9**, 2009–2016.

29 S. Ozaki, I. Kushida, T. Yamashita, T. Hasebe, O. Shirai and K. Kano, Inhibition of crystal nucleation and growth by water-soluble polymers and its impact on the supersaturation profiles of amorphous drugs, *J. Pharm. Sci.*, 2013, **102**(7), 2273–2281.

30 S. Ozaki, I. Kushida, T. Yamashita, T. Hasebe, O. Shirai and K. Kano, Evaluation of drug supersaturation by thermodynamic and kinetic approaches for the prediction of oral absorbability in amorphous pharmaceuticals, *J. Pharm. Sci.*, 2012, **101**(11), 4220–4230.

31 S. Xu and W. G. Dai, Drug precipitation inhibitors in supersaturable formulations, *Int. J. Pharm.*, 2013, **453**, 36–43.

32 S. A. Raina, B. Van Eerdenbrugh, D. E. Alonzo, H. Mo, G. G. Z. Zhang and L. S. Taylor, Trends in the precipitation and crystallization behavior of supersaturated aqueous solutions of poorly water-soluble drugs assessed using synchrotron radiation, *J. Pharm. Sci.*, 2015, **104**, 1981–1992.

33 D. B. Warren, C. A. Bergström, H. Benameur, C. J. Porter and C. W. Pouton, Evaluation of the structural determinants of polymeric precipitation inhibitors using solvent shift methods and principle component analysis, *Mol. Pharmaceutics*, 2013, **10**, 2823–2848.

34 J. L. Terebetski and B. Michniak-Kohn, Combining ibuprofen sodium with cellulosic polymers: a deep dive into mechanisms of prolonged supersaturation, *Int. J. Pharm.*, 2014, **475**, 536–546.

35 J. Anwar, P. K. Boateng, R. Tamaki and S. Odedra, Mode of action and design rule for additives that modulate crystal nucleation, *Angew. Chem., Int. Ed.*, 2009, **48**, 1596–1600.

36 G. A. Ilevbare, H. Liu, K. J. Edgar and L. S. Taylor, Maintaining supersaturation in aqueous drug solutions: impact of different polymers on induction times, *Cryst. Growth Des.*, 2013, **13**, 740–751.

37 F. Meng, A. Trivino, D. Prasad and H. Chauhan, Investigation and correlation of drug polymer miscibility and molecular interactions by various approaches for the preparation of amorphous solid dispersions, *Eur. J. Pharm. Sci.*, 2015, **71**, 12–24.

38 D. D. Sun and P. I. Lee, Probing the mechanisms of drug release from amorphous solid dispersions in medium-soluble and medium-insoluble carriers, *J. Controlled Release*, 2015, **211**, 85–93.

39 M. Maniruzzaman, D. J. Morgan, A. P. Mendham, J. Y. Pang, M. J. Snowden and D. Douroumis, Drug–polymer intermolecular interactions in hot-melt extruded solid dispersions, *Int. J. Pharm.*, 2013, **443**, 199–208.

40 X. Li, H. Peng, B. Tian, J. Gou, Q. Yao, X. Tao, H. He, Y. Zhang, X. Tang and C. Cai, Preparation and characterization of azithromycin – Aerosil 200 solid dispersions with enhanced physical stability, *Int. J. Pharm.*, 2015, **486**, 175–184.

41 M. J. Jackson, U. S. Kestur, M. A. Hussain and L. S. Taylor, Characterization of supersaturated danazol solutions—impact of polymers on solution properties and phase transitions, *Pharm. Res.*, 2016, **33**, 1276–1288.

42 W. Ali, A. C. Williams and C. F. Rawlinson, Stochiometrically governed molecular interactions in drug: Poloxamer solid dispersions, *Int. J. Pharm.*, 2010, **391**, 162–168.

43 Y. Lu, N. Tang, R. Lian, J. Qi and W. Wu, Understanding the relationship between wettability and dissolution of solid dispersion, *Int. J. Pharm.*, 2014, **465**, 25–31.

44 J. M. Miller, A. Beig, B. J. Krieg, R. A. Carr, T. B. Borchardt, G. E. Amidon, G. L. Amidon and A. Dahan, The solubility–permeability interplay: mechanistic modeling and predictive application of the impact of micellar solubilization on intestinal permeation, *Mol. Pharmaceutics*, 2011, **8**(5), 1848–1856.

45 J. M. Miller, A. Beig, R. A. Carr, G. K. Webster and A. Dahan, The solubility–permeability interplay when using cosolvents for solubilization: revising the way we use solubility-enabling formulations, *Mol. Pharmaceutics*, 2012, **9**(3), 581–590.

46 N. Otsuka, K. Ueda, N. Ohygi, K. Shimizu, K. Kataoka, T. Kumamoto, K. Higashi, K. Yamamoto and K. Moribe, An insight into different stabilization mechanisms of phenytoin derivatives supersaturation by HPMC and PVP, *J. Pharm. Sci.*, 2015, **104**, 2574–2582.